AFRL-DE-PS-
JA-2006-1001

AFRL-DE-PS-
JA-2006-1001

PERFORMANCE COMPARISON OF OPTICALLY PUMPED TYPE-II MID-INFRARED LASERS

A.P. Ongstad, et al.

25 October 2005

Journal Article

AIR FORCE RESEARCH LABORATORY
Directed Energy Directorate
3550 Aberdeen Ave SE
AIR FORCE MATERIEL COMMAND
KIRTLAND AIR FORCE BASE, NM 87117-5776

REPORT DOCUMENTATION PAGE

Form Approved
OMB No. 0704-0188

1. REPORT DATE *(DD-MM-YYYY)*	2. REPORT TYPE	3. DATES COVERED *(From – To)*
25 October 2005	Journal Article Postprint	1 August 2004 – 7 July 2005

4. TITLE AND SUBTITLE
Performance Comparison of Optically Pumped Type-II Mid-Infrared Lasers

5a. CONTRACT NUMBER
In-House (DF297213)

5b. GRANT NUMBER

5c. PROGRAM ELEMENT NUMBER
63605F

6. AUTHOR(S)
A.P. Ongstad, R. Kaspi
M.L. Tilton (Boeing Defense & Space Grp)
J.R. Chavez (Boeing Defense & Space Grp)
G.C. Dente (GCD Associates)

5d. PROJECT NUMBER
4866

5e. TASK NUMBER
LY

5f. WORK UNIT NUMBER
12

7. PERFORMING ORGANIZATION NAME(S) AND ADDRESS(ES)

8. PERFORMING ORGANIZATION REPORT NUMBER

9. SPONSORING / MONITORING AGENCY NAME(S) AND ADDRESS(ES)
Air Force Research Laboratory
3550 Aberdeen Avenue SE
Kirtland AFB, NM 87117-5776

10. SPONSOR/MONITOR'S ACRONYM(S)

11. SPONSOR/MONITOR'S REPORT NUMBER(S)
AFRL-DE-PS-JA-2006-1001

12. DISTRIBUTION / AVAILABILITY STATEMENT
Approved for public release; distribution is unlimited.

13. SUPPLEMENTARY NOTES
Published in Journal of Applied Physics **98**, 043108 (2005),

14. ABSTRACT
We report a comparative study on the performance of three optically pumped, type-II quantum well lasers with differing quantum well confinement. One of the active regions emphasized hole confinement, another emphasized electron confinement, while the third incorporated both electron and hole confinement. In all cases the wells were inserted in a thick $In_xGa_{1-x}As_ySb_{1-y}$ waveguide/absorber region. The lasing wavelengths at 84 K were 2.26 um, 3.44 um, and 2.37 um, respectively. The maximum peak output powers and differential quantum efficiencies, η, at 84 K were similar for the hole well and W lasers ($\approx$ 13 W, $\eta \approx 0.55$), but significantly reduced in the electron well only laser (2.3 W, $\eta = 0.14$). Waveguide loss measurements via the traditional quantum efficiency vs. cavity length method and by a Hakki-Paoli method revealed that all three lasers had low waveguide loss that either increased slowly or not at all with increasing temperature. However, the laser's internal efficiency, η_i, showed a linear decline with increasing temperature, with the η_i of the electron well only laser significantly less than the other two. The data suggests that for antimonide based type-II designs, strong hole confinement is essential for improved performance. The data further suggest that it is hole leakage from the QW and/or hole dilution that is largely responsible for the degradation in laser performance.

15. SUBJECT TERMS

16. SECURITY CLASSIFICATION OF:			17. LIMITATION OF ABSTRACT	18. NUMBER OF PAGES	19a. NAME OF RESPONSIBLE PERSON
a. REPORT	b. ABSTRACT	c. THIS PAGE			Dr. Andrew Ongstad
Unclassified	Unclassified	Unclassified	Unlimited	10	19b. TELEPHONE NUMBER *(include area code)*

Performance comparison of optically pumped type-II mid-infrared lasers.

A. P. Ongstad and R. Kaspi
Air Force Research Laboratory, Directed Energy Directorate, Kirtland AFB, Albuquerque, NM 87117

M. L. Tilton, J. R. Chavez
Boeing Defense and Space Group, Albuquerque, New Mexico 87106

G. C. Dente
GCD Associates, Albuquerque, New Mexico 87110

Abstract

We report a comparative study on the performance of three optically pumped, type-II quantum well lasers with differing quantum well confinement. One of the active regions emphasized hole confinement, another emphasized electron confinement, while the third incorporated both electron and hole confinement. In all cases the wells were inserted in a thick $In_xGa_{1-x}As_ySb_{1-y}$ waveguide/absorber region.. The lasing wavelengths at 84 K were 3.44 um, 2.26 um and 2.37 um, respectively. The maximum peak output powers and differential quantum efficiencies, η_i at 84 K were similar for the hole well and W lasers ($\approx$ 13 W, $\eta \approx 0.55$), but significantly reduced in the electron well only laser (2.3 W, $\eta = 0.14$). Waveguide loss measurements via the traditional quantum efficiency vs. cavity length method and by a Hakki-Paoli method revealed that all three lasers had low waveguide loss that either increased slowly or not at all with increasing temperature. However, the laser's internal efficiency, η_i, showed a linear decline with increasing temperature, with the η_i of the electron well only laser significantly less than the other two. The data suggests that for antimonide based type-II designs, strong hole confinement is essential to improved performance. The data further suggest that it is hole leakage from the QW and/or hole dilution that is largely responsible for the degradation in laser performance.

JOURNAL OF APPLIED PHYSICS 98, 043108 (2005)

Performance comparison of optically pumped type-II midinfrared lasers

A. P. Ongstad[a] and R. Kaspi
Air Force Research Laboratory, Directed Energy Directorate, Kirtland Air Force Base (AFB), Albuquerque, New Mexico 87117

M. L. Tilton and J. R. Chavez
Boeing Defense and Space Group, Albuquerque, New Mexico 87106

G. C. Dente
GCD Associates, Albuquerque, New Mexico 87110

(Received 22 February 2005; accepted 7 July 2005; published online 23 August 2005)

We report a comparative study on the performance of three optically pumped, type-II quantum well lasers with differing quantum well (QW) confinement. One of the active regions emphasized hole confinement, another emphasized electron confinement, while the third incorporated both electron and hole confinements. In all cases the wells were inserted in a thick $In_xGa_{1-x}As_ySb_{1-y}$ waveguide/absorber region. The lasing wavelengths at 84 K were 2.26, 3.44, and 2.37 μm, respectively. The maximum peak output powers and differential quantum efficiencies η at 84 K were similar for the hole well and W lasers ($\approx$13 W, $\eta \approx 0.55$), but significantly reduced in the electron-well-only laser (2.3 W, $\eta=0.14$). Waveguide loss measurements via the traditional quantum efficiency versus cavity length method and by a Hakki-Paoli method revealed that all three lasers had low waveguide loss that either increased slowly or not at all with increasing temperature. However, the laser's internal efficiency, η_i, showed a linear decline with increasing temperature, with the η_i of the electron-well-only laser significantly less than the other two. The data suggest that for antimonide-based type-II designs, strong hole confinement is essential for improved performance. The data further suggest that it is hole leakage from the QW and/or hole dilution that is largely responsible for the degradation in laser performance. © *2005 American Institute of Physics.* [DOI: 10.1063/1.2010627]

INTRODUCTION

Several transmission windows exist in the 2–10 μm region of the atmosphere, including relatively transparent regions near 2.0, 3.7, 4.2, and 9.0 μm. The development of mid-infrared (mid-IR) laser sources operating in these regions is useful in a number of applications, including infrared countermeasures and free space optical communication. In addition, the 2–10 μm region is part of the fingerprint region for molecular absorbance; for example, an important greenhouse gas, methane, shows a strong absorbance feature near 3.4 μm and is attributable to the C–H stretching vibration. Mid-IR laser applications geared toward chemical detection include industrial emissions monitoring, remote sensing, and medical diagnostics. For several of these applications, the laser requirements typically include high average power emission with good beam quality; this is especially true if the beam must be propagated several kilometers in distance.

Optically pumped semiconductor lasers (OPSELs) based on InAs/InGaSb/InAs, type-II quantum wells have demonstrated significant wavelength flexibility; by careful adjustment of the InAs layer thickness, the emission can be selectively and repeatedly tuned to any desired wavelength in the 2–10-μm region.[1–3] Over the past several years, a number of epitaxial design innovations to these type-II lasers have contributed to significant improvements in both beam quality and output power. These innovations include the addition of integrated absorber layers, in which the type-II wells are placed in a thick InGaAsSb waveguide engineered to efficiently absorb the pump radiation and create carriers.[4,5] Another important innovation was the formation of Al-free, dilute waveguide lasers, in which the optical confinement factor Γ is reduced.[6] Reduction in the confinement of the optical mode leads to a reduction in laser filamentation thereby improving the lateral divergence properties.[7] Finally, the incorporation of increased compressive strain in the hole-bearing $In_xGa_{1-x}Sb$ layer by increasing the In mole fraction x has been demonstrated to be beneficial. The increased strain splits the degeneracy of the light and heavy hole band at the valence-band maximum and also improves hole confinement. Devices with $0.25 \leqslant x \leqslant 0.45$ have shown improved thermal properties, i.e., larger T_0 and T_1 values.[8]

Despite the improvements observed in quantum efficiency, output power, and divergence, operation at higher temperatures remains problematical. The temperature sensitivity of the laser threshold T_0 and the temperature sensitivity of the laser slope efficiency T_1 are sound indicators of thermal robustness with higher values being more desirable. Typical T_0 and T_1 values for these lasers are ~45 and ~60 K, respectively. In comparison, near-IR-emitting InGaAs diodes have much higher T_0 and T_1 values of >200 and >500 K, respectively.[9] Several recent studies on antimonide-based mid-IR lasers have begun to shed light on

[a]Electronic mail: andrew.ongstad@kirtland.af.mil

the causes of the temperature degradation observed in these lasers. A recent study in this laboratory has suggested that these dilute waveguide, type-II W lasers have very low waveguide loss that does not increase significantly as the temperature is raised.[10] However, a rapid decrease in the laser internal efficiency η_i was observed as the temperature was increased. In an experiment in which the pump power was fixed, a rapid linear falloff in the peak gain was observed as the temperature was increased from 100 to 130 K.[10] Gain calculations based on a superlattice empirical pseudopotential method (SEPM) were able to accurately predict the gain falloff by assuming a modest reduction in the carrier density.[10] However, more interestingly, the SEPM, for a case in which the inversion was fixed, revealed an inherent decrease in the gain with increasing temperature. We attributed this type of gain reduction to the large differences between the valence and conduction subband curvatures that naturally exist in these W lasers. This fixed inversion gain reduction is independent of nonradiative recombination mechanisms, such as Auger and Shockley-Reed.

In a related study on a 3-μm electrically injected W quantum well laser the performance degradation with temperature was, again, not attributable to a runaway waveguide loss; the waveguide loss was shown to be nearly independent of temperature in the range from 80 to 160 K. The study also looked at the spontaneous emission intensity as a function of increasing current density at the two temperatures. At the higher temperature a region was observed where the spontaneous emission intensity showed a 2/3 power dependence on current density. Such a dependence suggests that the main contribution to the temperature dependence of the threshold current was Auger recombination.[11] Also, in a recent comparative study of the temperature sensitivity of mid-IR type-I and type-II lasers it was shown that the temperature decay of the photoluminescence is generally stronger in structures with low hole confinement and greater in type-II than in type-I heterostructures.[12]

To provide more insight into the thermally induced degradation mechanisms in type-II lasers, we have investigated the performance of three fundamental, antimonide-based active regions. The active regions included either an InAs electron well, an InGaSb hole well, or an InAs/InGaSb/InAs W well in which the InAs layers were held to a single monolayer thickness. In all cases, the quantum wells are periodically inserted between thick $In_xGa_{1-x}As_ySb_{1-y}$ waveguides. Waveguide loss measurements conducted by a Hakki-Paoli measurement and by standard-length study measurements indicate either no increase in waveguide loss or a modest increase in waveguide loss as temperature is raised. These measurements are in agreement with the results presented in Ref. 11. Thus, the decreasing external quantum efficiency that is observed in these lasers is largely the result of a decline in the laser's internal efficiency as the temperature is raised. Further, for the laser structure in which only the electrons are quantum confined, the internal efficiency is further degraded; even at cryogenic temperatures the internal efficiency is less than 40%. In contrast, the device in which only the holes are quantum confined has a much larger internal efficiency of 90%. These results suggest that strong hole confinement is a key to producing more thermally tolerant devices.

EXPERIMENT

Lasers were epitaxially grown in our laboratory by using a commercial solid-source molecular-beam epitaxy (MBE) system, configured specifically for antimonide alloy deposition. Heterostructures were deposited on two-inch-diameter (001)-oriented GaSb:Te substrates. Three laser designs were fabricated. The designs incorporate either 6 or 14 type-II quantum wells which are placed between 1000-Å-thick quaternary layers composed of InGaAsSb (~20% In). These thick layers serve as both waveguide and highly effective pump absorbance layers. For example, in the 6- and 14-quantum-well designs with thicknesses of 7126 and 15,336 Å the absorbances at the pump wavelength are ~0.48 and ~0.76, respectively.

The following type-II quantum wells were periodically inserted between the thick InGaAsSb quaternary layers: (a) an ~18-Å-thick $In_{0.35}Ga_{0.65}Sb$ hole-bearing layer; (b) an ~24-Å-thick InAs electron-bearing layer; and (c) an ~24-Å-thick $In_{0.35}Ga_{0.65}Sb$ hole-bearing layer sandwiched by two ultrathin, ~3-Å InAs-coupled electron wells. Hence, lasers (a)–(c) nominally comprise a quaternary-ternary (QT) laser with no deliberate electron confinement, a quaternary-binary (QB) laser with no deliberate hole confinement, and a short wavelength W laser with both electron and hole confinements, respectively. The QB laser differs from the other two in that it has only 6 quantum wells, not 14, and instead of GaSb cladding layers, incorporates an aluminum-bearing optical clad with an approximate composition of $Al_{0.9}Ga_{0.1}As_{0.09}Sb_{0.91}$. The QB laser is more fully described in Ref. 13. The optical clad in the QT and W lasers is GaSb, which has a much smaller index step relative to the quaternary waveguide and provides for a reduced optical confinement. These "dilute waveguides" have a number of benefits including a lower tendency to self-focus or form filaments; consequently low confinement structures show improved lateral beam quality as well as other benefits.[6,7]

The laser devices' optical and thermal characterization was carried out by placing small wafer sections into a variable temperature cryostat and optically exciting the sample with a high-power 1.93-μm laser diode array (LDA) that has been described previously.[1,8] In brief, wafer sections were lapped and polished to ~150-μm thickness and pieces were cleaved to form either, 1.0, 1.5, 2.0, or 2.5-mm-long cavities. The samples were In soldered, epi-side up, to a final gold-plated copper heat sink and placed in a LN2 dewar. A high-power LDA was used as the optical excitation source and illuminated a 250-μm-wide stripe [full width at half maximum (FWHM)] traversing the laser bar. All measurements employed a 32-μs pump pulse duration at a 1% duty cycle. Output power measurements were performed by collecting the emission from one facet using a gold-coated ellipsoidal mirror and focusing it onto a thermal detector.

Initial spectral measurements were made by focusing the laser output onto the entrance slit of a 0.25-m monochro-

mator. A long-pass-filter was placed at the entrance slit to remove any residual pump radiation and any photoluminescence originating in the substrate. A 150-groove/mm grating was used to disperse the near-IR radiation which was detected with a LN2-cooled InSb photodiode. The signal was amplified and passed to a gated integrator/boxcar averager for final signal processing.

Measurements of waveguide loss using a Hakki-Paoli below the band-gap measurement technique utilized a Nicolet Magna 760 Fourier transform infrared (FTIR) spectrometer as previously described.[10] In brief, the waveguide loss may be estimated from the gain values calculated from the low-energy side of the spectrum, where the small signal gain g approaches zero. In this circumstance, $g \sim 0$, and the simplified expression for the single-pass power gain, $G=\exp(g-a)L \approx \exp(-aL)$, gives the waveguide loss a for a cavity length L as $a \approx -\ln(G)/L$. The gain G was determined by a full-curve fit of the spectral data to the following function, which gives the spectral output (S) of a Fabry-Perot cavity modified to include the effects of any incoherent background:

$$S = \frac{C}{[1 + (RG)^2 - 2RG\cos\,\delta]} + \eta. \tag{1}$$

Here, R represents the modal facet power reflectivity, $\delta = 4\pi\bar{n}L/\lambda$, where $\bar{n}$ is the modal index, L is the device length, λ is the device wavelength, C is an amplitude-scaling factor, and η accounts for any incoherent background emission. This derivation assumes a single lateral and transverse mode propagating between the facets, with $RG=1$ corresponding to the laser threshold. The parameters C, RG, δ, and η are adjusted until Eq. (1) agrees with the measured data.

The full-curve fit procedure is preferable to the gain determination via the peak to valley method in cases where good lateral mode filtering cannot be employed and an appreciable incoherent background is present. In such instances Eq. (1) still yields accurate G values whereas the peak to valley method will be compromised with the error increasing with increasing background.[10]

RESULTS AND DISCUSSION

Figure 1 shows the SEPM calculated probability density of both electrons and holes in the (001) growth direction as a function of position in one period of the structure for all three lasers. These probability densities are calculated for flatband conditions. The SEPM method of calculating band structure and carrier wave functions in coherently strained periodic structures is described in detail elsewhere.[14,15] The calculations reveal that in the QT laser, the holes are quantum confined in the ternary InGaSb layer, and the electrons are nominally unconfined in the thick quaternary layer. In contrast, the QB laser represents the reverse carrier confinement situation. In this case, the electrons are quantum confined in the InAs and the holes are nominally unconfined; the holes are found in the bulklike quaternary layer in which the valence states are very closely spaced. In the QT and QB structures, the electron and hole wave functions, respectively,

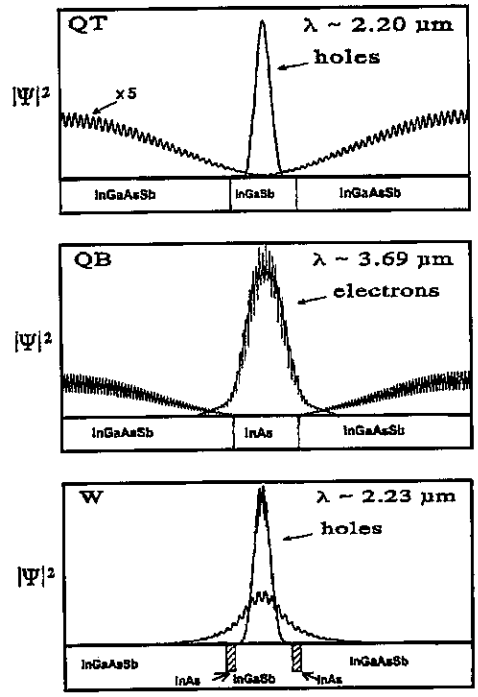

FIG. 1. Top panel: Calculated electron and hole densities for the quaternary-ternary (QT) laser, the quaternary-binary (QB) laser, and the W laser.

are concentrated at the center of the quaternary layer away from the heterointerface. Finally, in the W laser, with very thin InAs layers surrounding the InGaSb layer, both electrons and holes are quantum confined largely in the ternary layer. The electrons in the ultrathin InAs layers form a highly coupled well such that the electron wave function is spread over the hole-bearing ternary layer. In essence, the lowest-energy conduction-band-to-valence-band transition in this laser is effectively type I.

In the QB and QT lasers when the carrier density N_s is increased, Coulombic attraction or band bending pulls the carrier distribution in the quaternary layer toward the heterointerface. For example, in the QB laser, as N_s is increased from 0 to 5×10^{10} cm^{-2}, an ~20-meV voltage dip is induced at the quaternary-binary interface and forms a shallow well for the electrons. Furthermore, the radiative matrix element increases significantly from 3872 eV Å to 15,603 eV Å, respectively. The band-bending results in a small calculated blue shift of the emission wavelength from 3.69 to 3.52 μm. The blueshift has been observed in an experiment in which the photoluminesence spectrum was monitored as a function of pumping.[13]

The SEPM-calculated wavelengths, not including the effects of band bending, for the lowest-energy conduction-band-to-valence-band transition in the QT, QB, and W are 2.20, 3.69, and 2.23 μm, respectively. These values are in good agreement with the measured wavelength values of 2.26, 3.44, and 2.38 μm. Figure 2 shows the spectra collected at 84 K at an absorbed pump power of ~13 W. These spectra are multimode, with a $1/e^2$ full width of ~5.3 meV. Figure 3 shows the power-power curves collected for 2.5-mm-long devices. Similar, double-ended peak output power curves were obtained on the QT and the W lasers. The maxi-

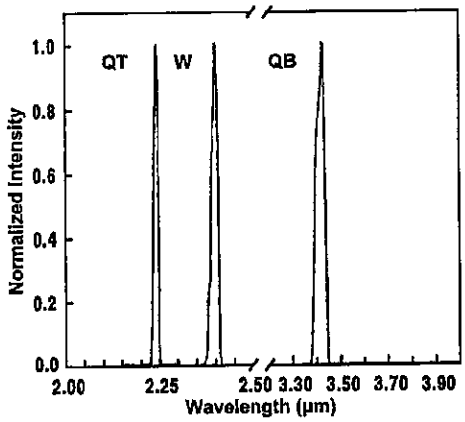

FIG. 2. Lasing spectra for the three laser sources.

mum power extracted from these lasers was near 13 W and was limited by the availability of pump power. Both lasers also show a very low threshold fluence of <50 W cm^{-2} and relatively high differential quantum efficiencies η of $>50\%$. In order to determine the T_0 and T_1 values, the power-power curves were collected as a function of increasing temperature from 90 to $\sim$230 K. T_0 values of 54 and 40 K, and T_1 values of 137 and 112 K were obtained for the QT and W lasers, respectively. Figure 4(a) plots the differential quantum efficiency as a function of temperature. The performance of the QT and W lasers is similar. In contrast, the overall performance of the QB laser is markedly inferior to that of the QT and W. Figure 3 shows that much less power is obtained from this laser, $\approx$2 W, and the resultant quantum efficiency, even at 84 K, is only 14%. Figure 4(a) compares the QB performance with that of the other two lasers. Its quantum efficiency is significantly lower, and lasing terminates near 150 K, where $\eta<3\%$. At 150 K the power output from the QT and W is still $\approx$4.5 W with a $\eta>40\%$. Moreover, the T_0 and T_1 values for the QB of 24 and 49 K are noticeably smaller than for the other two lasers. Table I summarizes the characterization results for all three lasers.

Certainly, the QT and W lasers are much more thermally robust than the QB. Furthermore, the QT appears more thermally tolerant than the W. This is surprising, since the W laser structure confines both electrons and holes, but the QT confines only the holes. In order to obtain a more complete understanding of the mechanisms limiting the thermal performance of these lasers we have measured the waveguide loss a and internal laser efficiency η_i as a function of temperature. By cleaving different cavity length lasers and measuring the differential quantum efficiency η_d as a function of length, the internal efficiency and waveguide loss may be determined using

$$\eta^{-1} = \eta_i^{-1}\left[\frac{2La}{-\ln(R_f R_b)} + 1\right], \tag{2}$$

where R_f and R_b are the front and back mirror reflectivities. Figure 5 plots the waveguide loss as a function of heat sink temperature and shows that all the lasers at 90 K have relatively low waveguide loss values ranging from $\approx$2 to $\approx$4 cm^{-1}. For the QT and W lasers, a moderate linear increase in the waveguide loss is observed as the temperature is raised. The data indicate that for a 100-K increase in temperature, the waveguide loss increases by 2.3 and 3.6 cm^{-1} for the QT and W lasers, respectively. The QB laser shows no increase in waveguide loss up to 130 K; the waveguide loss remains near $\approx$4 cm^{-1} over the sampled interval. Figure 5 also shows the waveguide loss results determined via the Hakki-Paoli method which employed a full-curve fit to Eq. (1) over a spectral interval in the band gap; these results are in good agreement with the results from the quantum efficiency versus length study.

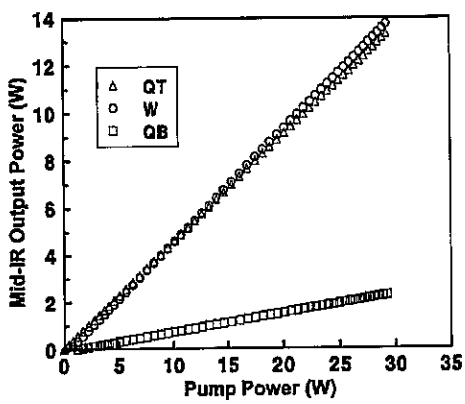

FIG. 3. Absorbed 1.9-μm pump power vs mid-IR output power for the three laser sources.

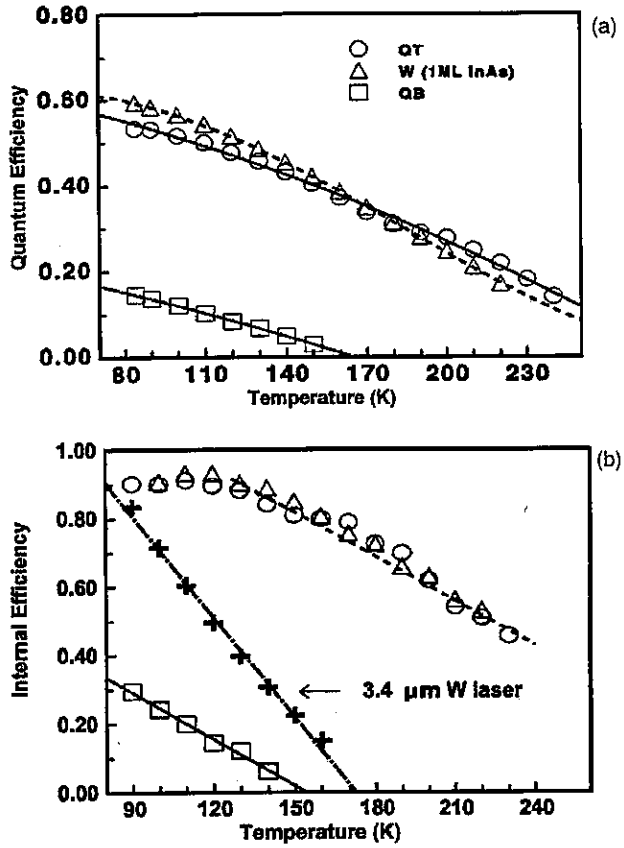

FIG. 4. (a) Double-ended quantum efficiency vs temperature for the three lasers. (b) Laser internal efficiency vs temperature. The results for a 3.4 μm W laser are also shown.

TABLE I. InAs/InGaSb/InAs type-II quantum well lasers.

Type	λ (um)	InAs thickness (ML)	InGaSb thickness (ML)	P_{max} (W)[a]	Spectral width[a] ($1/e^2$, meV)	$\eta^{a,b}$	Threshold[a] (W cm^{-2})	T_0 (K)	T_1 (K)	$\Theta_\perp$[c]	$\Theta_\parallel$[c]
QT	2.26	0	8	13.25	5.00	0.53	40	54	137	24.5	11.8
W	2.37	1	8	13.70	5.65	0.59	40	40.4	112	19.3	6.8
QB	3.44	8	0	2.28	5.44	0.14	16	24	49	···	···

[a]Measured at 84 K.
[b]Double-ended quantum efficiency.
[c]Divergence measured in degrees at the FWHM points. The cavity length and width of all lasers was 0.25 and 0.025 cm, respectively.

The low waveguide loss values are consistent with measurements made previously on an InAs/InGaSb/InAs W laser emitting near 3.4 μm.[10] In that study, a waveguide loss of 2.7 cm^{-1} was measured at 78 K, with no increase observed at 120 K. These low waveguide losses suggest that intervalence-band absorbance and free-carrier absorbance are not the primary or dominant mechanisms driving down the quantum efficiency with increasing temperature. Rather, it is the decline in internal efficiency with temperature that accounts, largely, for the decreasing η performance. The length studies reveal that all three lasers show a decreasing internal efficiency with increasing temperature, as can be seen in Fig. 4(b), which plots the internal efficiency versus temperature. From the figure, it is apparent that the η_i of the QB laser is severely reduced when compared to the QT and W; at 90 K the η_i for the QB is only 0.3, while for the QT and W lasers $\eta_i > 0.85$. This decrease in η_i is not simply due to the larger quantum defect of the QB, since the 3.4-μm W laser with a near equivalent quantum defect also has $\eta_i > 0.83$ at 90 K.

Why is the performance of the QB so much worse than that of the QT? Figure 6 displays a qualitative band-bending diagram for the two lasers. In both lasers, Coulomb attraction pulls carriers toward the interface resulting in the band structure shown. However, since the effective hole mass is much greater than the effective electron mass ($m_h \gg m_e$) the valence-band states are much more densely packed near the band edge in the QB than are the conduction-band states in the QT. Hence, in the QB, the gain is diluted over a much larger density of states which is manifested in the poor η_i. This is supported by the data shown in Fig. 7. This figure plots the results of an experiment in which the peak laser gain was measured as a function of temperature at a fixed pumping power. The upper three curves give the results for the QT, QB, and W for equivalent pump power per quantum well, 20 mW/well. The lowest curve gives the results for a 14-quantum-well, dilute waveguide, QB laser that had an emission wavelength near 3 μm. This QB_{dilute} was pumped at a higher power of 76 mW/well. The dilute waveguide laser was grown to provide a more directly comparable test structure to the QT. The QB_{dilute} had the same number of QW's and the same low confinement waveguide as the QT and W.

From Fig. 7 it is apparent that the QT displays the highest gain at a particular temperature and that the QB_{dulute} displays the lowest gain. In fact, the QB_{dilute} barely exceeds transparency at 79 K. Furthermore, to reach $g=7$ cm^{-1} the QB_{dilute} would need to be cooled to ≈42 K compared to 118 K for the QT. This indicates that considerable thermal energy must be removed from the QB_{dilute} in order to reach approximately half the threshold gain value. Not surprisingly, we were unable to get the QB_{dilute} to lase even with significantly higher pump excitation. Thus, the more directly comparable laser structure, the QB_{dilute}, demonstrates, in

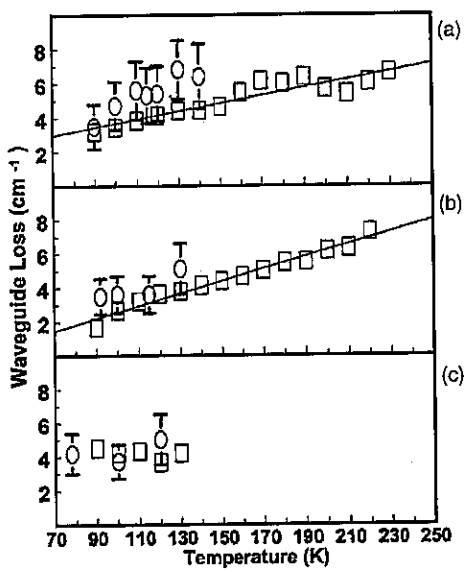

FIG. 5. Waveguide loss vs temperature for (a) the QT laser, (b) the W laser, and (c) the QB laser. The circles are from the Hakki-Paoli derived waveguide loss measurements and the squares are from the waveguide loss determined using Eq. (2).

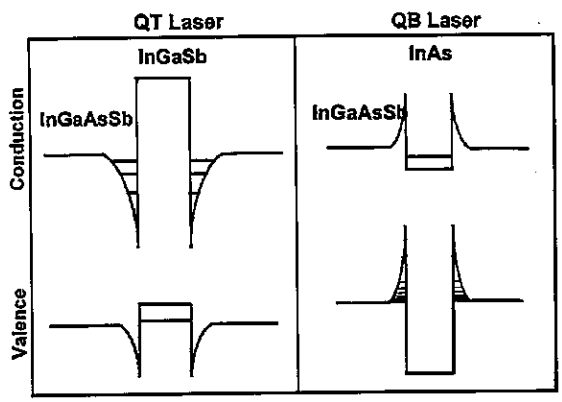

FIG. 6. Qualitative band-bending diagrams for the QT and QB lasers.

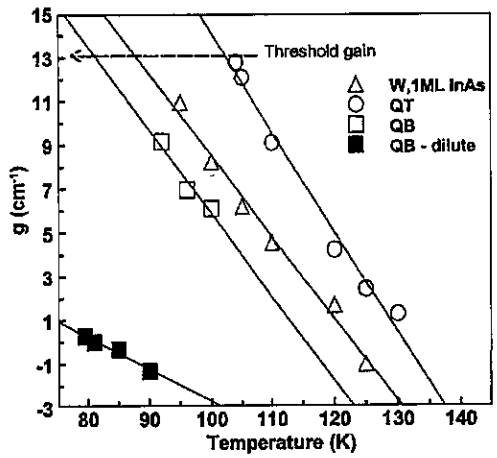

FIG. 7. Small signal gain vs temperature for the QT, QB, and W. Also shown are the results for a QB structure containing 14 quantum wells in a low confinement optical waveguide, i.e., the QB_{dilute}. The QB_{dilute} was grown to provide a more directly comparable test structure to the QT and W lasers. The QB_{dilute} had the same number of QW's and the same low confinement waveguide as the QT and W lasers. The dashed line gives the approximate gain value required to reach threshold.

even starker terms, the consequence of not confining the holes, i.e., laser action, even at cryogenic temperatures, is not possible in a dilute waveguide structure.

Overall, the results suggest that an effective hole quantum well is essential in producing a larger η_i and hence a larger η. Without hole quantitization, or where the hole density of states are bulklike, the performance is significantly degraded. Somewhat unexpectedly, the data also suggest that adding electron confinement does not enhance performance, since the QT laser performed as well as, if not better than, the W laser. This may be due to a reduced hole transport through the InAs layer, which effectively acts as a barrier through which the holes must tunnel. Certainly, hole transport issues are expected to be exacerbated in the longer-wavelength W lasers which have a thicker InAs layer.

The importance of the hole quantum well to laser performance indicates that the η_i degradation mechanisms in W lasers are largely traceable to loss mechanisms and transport mechanisms associated with the hole well.One nonradiative loss mechanism has been suggested by subthreshold gain data measurements at fixed pumping and SEPM modeling of fixed-inversion peak gain-versus-temperature data for a 3.4-μm W laser.[10] The SEPM data are displayed in Fig. 8; the data shows an intrinsic gain reduction independent of nonradiative loss mechanisms, such as Auger and Shockley-Reed. We attribute this gain reduction to the large differences between the valence and conduction subband curvatures. In particular, the flatter valence subbands allow the holes to spread significantly in the in-plane phase space, so that the number of directly radiatively connected electrons and holes are reduced. This "hole dilution" process leads to an appreciable reduction in gain as the temperature is increased. Furthermore, as the operational wavelength of the W laser is increased to 7.3 μm, by increasing the InAs layer thickness to $\approx$10 monolayers (MLs), the SEPM gain falloff is even more pronounced. This is due to increased hole dilution and more than one conduction state being populated as, for example, when the electron well is widened and the conduction-band states become quasidegenerate. In addition, reduced hole transport is likely as the InAs layer is thickened and would be expected to yield lower gain values for the longer-wavelength device. Indeed, these effects are reflected in the η versus temperature plots for the 3.4-μm (T_1 =53 K) and 7.3-μm (T_1=31 K) W lasers and are indicative of the general trend of decreasing T_1 values in the W lasers with increasing wavelength.

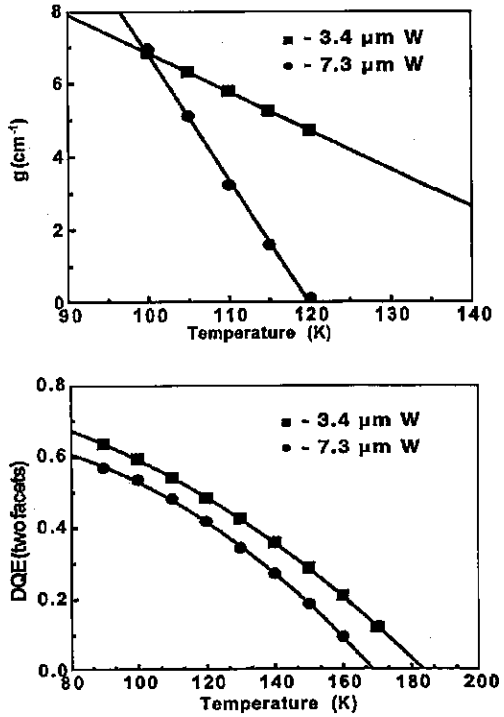

FIG. 8. SEPM-calculated small signal gain vs temperature for a 3.4- and 7.3-μm W laser. Measured differential quantum efficiency vs temperature for the 3.4- and 7.3-μm W lasers.

CONCLUSIONS

Three primary mid-IR quantum well active regions have been investigated. The active regions included either an InAs electron well, an InGaSb hole well, or an InAs/InGaSb/InAs W well in which the InAs layers were held to a single monolayer thickness. In all cases, the quantum wells are periodically inserted between thick $In_xGa_{1-x}As_ySb_{1-y}$ layers that are highly efficient with $\sim$1.9-μm pump absorber regions. Waveguide loss measurements conducted by a Hakki-Paoli measurement and by standard length study measurements indicate either a modest increase in waveguide loss or no increase in waveguide loss as temperature is raised. For example, for the QT, W, and QB lasers the waveguide loss was observed to increase by 0.023 and 0.036 cm^{-1} K^{-1} over a 130-K interval and $\approx$0 cm^{-1} K^{-1} over a 50-K interval. Consequently, the decreasing external quantum efficiency that is observed in these lasers is largely the result of a decline in the lasers internal efficiency as the temperature is raised. The poor η_i and low T_1 value of the electron-only quantum well device, the QB, is due to the gain dilution incurred by the large density of valence-band states. In contrast, the much

higher η_i and T_1 values of the hole-only quantum well laser, the QT, is due to hole quantum confinement and the lower density of bound conduction-band states near the InGaAsSb/InGaSb heterointerface. The reduction in injection efficiency of the QT and W lasers with increasing temperature is partially the result of hole dilution, in which the momentum spread of the electrons in the conduction band does not match the larger momentum spread of the holes in the valence band. For W lasers in general, the η is decreased with longer-wavelength operation. The data suggest that this is due to increased hole dilution, more than one conduction state being populated as the electron well is widened, and reduced hole transport through the thicker InAs layers.

[1]R. Kaspi, A. P. Ongstad, G. C. Dente, M. L. Tilton, J. R. Chavez, and D. M. Gianardi, Appl. Phys. Lett. (submitted).
[2]I. Vurgaftman, C. L. Felix, W. W. Bewley, D. W. Stokes, R. E. Bartolo, and J. R. Meyer, Philos. Trans. R. Soc. London, Ser. A **359**, 489 (2001).
[3]W. W. Bewley *et al.*, OSA Trends in Optics and Photonics, Topical Meeting on Advanced Semiconductor Lasers and their Applications, Santa Barbara, CA, 21–23 July 1999 (unpublished), Vol. 31, pp. 158–160.
[4]A. K. Goyal, G. W. Turner, H. K. Choi, P. J. Foti, M. J. Manfra, T. Y. Fan, and A. Sanchez, Proceedings of Lasers and Electro-Optics Society (LEOS) Annual Meeting, 2000, Puerto Rico (unpublished), p. 249.
[5]G. W. Turner, M. J. Manfra, H. K. Choi, A. K. Goyal, S. C. Buchter, S. D. Calawa, A. Sanchez, and D. L. Spears, Symposium on Infrared Applications of Semiconductors III, Boston, MA, USA 29 November–2 December 1999 (unpublished); Symposium on Infrared Applications of Semiconductors III, Boston, MA, 29 November–2 December 1999 (unpublished), pp. 3–10.
[6]A. K. Goyal, G. W. Turner, M. J. Manfra, P. J. Foti, P. O'Brien, and A. Sanchez, Conference Proceedings of the Lasers and Electro-Optics Society Annual Meeting (LEOS), 14th Annual Meeting of the IEEE Lasers and Electro-Optics Society, San Diego, CA, 11–15 November 2001 (unpublished), pp. 200–201.
[7]G. C. Dente, IEEE J. Quantum Electron. **37**, 1650 (2001).
[8]A. P. Ongstad, R. Kaspi, J. R. Chavez, G. C. Dente, M. L. Tilton, and D. M. Gianardi, J. Appl. Phys. **92**, 5621 (2002).
[9]J. J. Lee, L. J. Mawst, and D. Botez, Electron. Lett. **39**, 1250 (2003).
[10]A. P. Ongstad, R. Kaspi, C. E. Moeller, M. L. Tilton, J. R. Chavez, and G. C. Dente, J. Appl. Phys. **95**, 5621 (2004).
[11]S. Suchalkin, D. Westerfeld, D. Donetski, S. Luryi, G. Belenky, R. Martinelli, I. Vurgaftman, and J. Meyer, Appl. Phys. Lett. **80**, 2833 (2002).
[12]S. Suchalkin, L. Shterengas, M. Kisin, S. Luryi, G. Belenky, R. Kaspi, A. Ongstad, J. G. Kim, and R. U. Martinelli, Appl. Phys. Lett. **87**, 041102 (2005).
[13]R. Kaspi, A. Ongstad, C. Moeller, G. C. Dente, J. Chavez, M. L. Tilton, and D. Gianardi, Appl. Phys. Lett. **79**, 302 (2001).
[14]G. C. Dente and M. L. Tilton, J. Appl. Phys. **86**, 1420 (1999).
[15]G. C. Dente and M. L. Tilton, Phys. Rev. B **66**, 165307 (2002).